analytical chemistry

Article

pubs.acs.org/ac

Asymmetric Signal Amplification for Simultaneous SERS Detection of Multiple Cancer Markers with Significantly Different Levels

Sujuan Ye,[†,‡] Yanying Wu,[‡] Xiaomo Zhai,[‡] and Bo Tang*[,†]

[†]College of Chemistry, Chemical Engineering and Materials Science, Collaborative Innovation Center of Functionalized Probes for Chemical Imaging in Universities of Shandong, Key Laboratory of Molecular and Nano Probes, Ministry of Education, Shandong Provincial Key Laboratory of Clean Production of Fine Chemicals, Shandong Normal University, Jinan 250014, P.R. China

[‡]Key Laboratory of Sensor Analysis of Tumor Marker Ministry of Education, College of Chemistry and Molecular Engineering, Qingdao University of Science and Technology, Qingdao 266042, P.R. China

Supporting Information

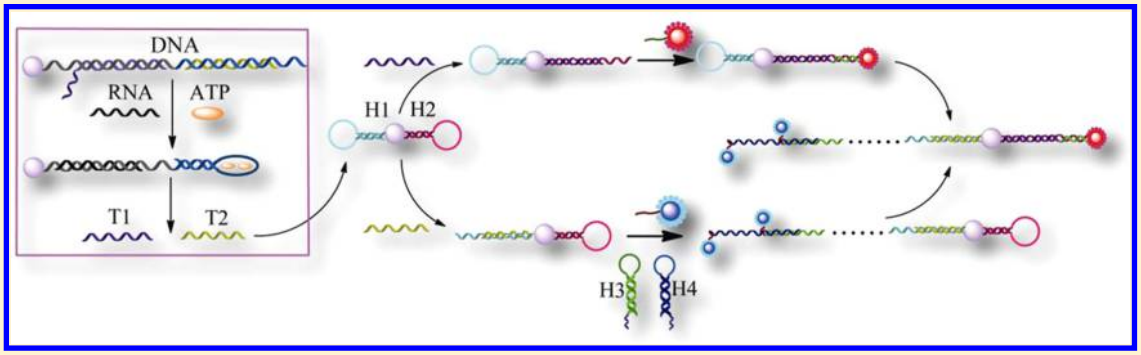

ABSTRACT: Simultaneous detection of cancer biomarkers holds great promise for the early diagnosis of different cancers. However, in the presence of high-concentration biomarkers, the signals of lower-expression biomarkers are overlapped. Existing techniques are not suitable for simultaneously detecting multiple biomarkers at concentrations with significantly different orders of magnitude. Here, we propose an asymmetric signal amplification method for simultaneously detecting multiple biomarkers with significantly different levels. Using the bifunctional probe, a linear amplification mode responds to high-concentration markers, and quadratic amplification mode responds to low-concentration markers. With the combined biobarcode probe and hybridization chain reaction (HCR) amplification method, the detection limits of microRNA (miRNA) and ATP via surface-enhanced Raman scattering (SERS) detection are 0.15 fM and 20 nM, respectively, with a breakthrough of detection concentration difference over 11 orders of magnitude. Furthermore, successful determination of miRNA and ATP in cancer cells supports the practicability of the assay. This methodology promises to open an exciting new avenue for the detection of various types of biomolecules.

Molecular biomarkers, including microRNA (miRNA), small bioactive molecules, and proteins, play critical regulatory functions in many biological processes, such as cell differentiation and cell apoptosis.[1−4] Therefore, sensitive detection of these biomarkers plays a critically important role in the early detection of cancer.[5−8] Substantial research efforts have recently been directed toward the highly sensitive detection of these cancer biomarkers. Several sensitive methods have been utilized for miRNA detection, including the isothermal signal amplification assays.[9−13] Although significant progress has been made over the past decade in analyzing a single biomarker, monitoring of a single biomarker is often not sufficient to diagnose the disease and follow its status. Simultaneous monitoring of multiple analytes is thus desired. In addition, compared with single-analyte assays, multiplexed analyses could offer several potential advantages in terms of improved detection efficiency, simplified analytical procedures, and reduced cost.[14] Furthermore, in clinical analysis, the simultaneous determination of panels of tumor markers has important application in the screening and diagnosis of cancer.[15,16] The possibility of monitoring more than one biomarker is known to enhance the accuracy of cancer diagnostics.[17,18] Therefore, much attention has been paid to the simultaneous detection of cancer biomarkers. CD44+/CD24+ subpopulations of cancer stem cells have been detected in three different breast cancer cell lines by constructing DNA−gold nanoparticle reversible networks.[19] Tang et al. developed multiple color nanoprobes that can simultaneously detect and image multiple miRNAs in living cells.[20−22] Nakano et al. achieved the simultaneous detection of ATP and GTP by covalently linked fluorescent ribonucleopeptide sensors.[23]

Received: March 29, 2015
Accepted: July 28, 2015
Published: July 28, 2015

DOI: 10.1021/acs.analchem.5b01186
Anal. Chem. 2015, 87, 8242−8249

Table 1. Oligonucleotide Sequences Used in Our Experiments

oligonucleotide name	sequences (5′ to 3′)
DNA1	NH_2CTAGTGGTCCTAAACATTTCACACCTGGGGGAGTATT GCG GAGGAAGGT
MiR-203	GUGAAAUGUUUAGGACCACUAG
trigger 1 (T1)	GTTTAGGACCACTTTAC
trigger 2 (T2)	TCCGCAATACTCCCCCA
H1 (complementary to T1, Scheme 1A)	NH_2TTTTTTCCTCTCGTAAAGTGGTCCTAAACGAGAGGGAAAGAGAGAG
H2 (complementary to T2, Scheme 1A)	NH_2TTTTTTTCTGGGGGAGTATTGCGGACTTCAGACTCCGCAATACT
H3 (helper strand, Scheme 1A, underline means sticky end)	CTCTCTCTCTTTCCCTCTCTTCGGCTTGAGAGGGAAAG *TCAAGTACAGC*
H4 (helper strand, Scheme 1A, underline means sticky end)	*TCAAGTACAGC*GAGAGGGAAAGAGAGAGAGCTTTCCCTCTCAAGCCGAA
H5 (helper strand, Scheme 2B, underline means sticky end)	TCATCTTCCTCTAACGACGCTTCAGACCGTCGTTAGAG*TCCGCAATACT*
H6 (helper strand, Scheme 2B, underline means sticky end)	*TCCGCAATACT*CGTCGTTAGAGGAAGATGACTCTAACGACGGTCTGAAG
H7 (complementary to T2, Scheme 2B)	NH_2TTTTTTTCGTAAAGGCTGTACTTGACACTCTGATCAAGTACAGC
H8 (complementary to T1, Scheme 2A)	NH_2TTTTTTACGACGGTGGGGGAGTATTCCGGACCGTCGTTAGAGCTTCAT
capture probe 1 (C1)	SH-AGTATTGCGGA
capture probe 2 (C2)	SH-GCTGTACTTGA
signal DNA 1	Rox-TTTTTTCCTAGCGAC-SH
signal DNA 2	Cy3-TTTTTTCCTAGCGAC-SH

Despite these achievements, current simultaneous detection schemes are always limited to the sensitive detection of target homologues with concentration levels similar to those present in the organism. However, to the best of our knowledge, the sensitive simultaneous detection of various types of biomarkers that differ in concentration by several orders of magnitude has never been reported. The sensitive and simultaneous detection of cancer biomarkers with great differences in concentration levels pose a great challenge in any detection method. First, contribution to the leveling effect of resolution, the signals of high-concentration analytes often overlap the signals of lower expression analytes.[24,25] Furthermore, under conditions where low-concentration biomarkers can be detected, signals from high-concentration biomarkers are saturated in the case of techniques such as DNA microarray, enzyme-linked immuno sorbent assay (ELISA), polymerase chain reaction (PCR), and nanopartical-based detection.[26−32] Finally, analytes present in high concentration levels always occupy the effective sensing interface and thus suppresses the sensing of other analytes. Thus, the simultaneous and sensitive detection of the biomarkers remains one of the major challenges for any detection method, irrespective of whether signal amplification is performed.

To overcome this limitation and further improve the accuracy of early cancer detection, we developed a new asymmetric signal amplification strategy for the simultaneous detection of biomarkers with significantly different levels. A linear amplification mode responds to high-concentration biomarkers, and a multiple-amplification mode responds to low-concentration markers. Several DNA amplification techniques have been developed through amplification of trace amounts of a specific sequence to levels that are detectable; these techniques include PCR,[33,34] rolling circle amplification (RCA),[35−37] and DNA strand displacement polymerization.[38−40] However, these methods use a single signal amplification mode. In this work, a bifunctional probe is assembled and asymmetric signal amplification is triggered on the probe. For instance, miR-203 expression levels are often low, and the amount of ATP is also relatively high in cells and circulating blood.[41−45] Coupling of SERS technology with hybridization chain reaction (HCR) amplification enabled the simultaneous detection of miR-203 and ATP, which are two important biomarkers.[46−50] The presence of the target ATP results in linear signal amplification, whereas the presence of the target miRNA initiates quadratic signal amplification. For this multiplex assay, the measurement precision was improved. Through the asymmetric signal amplification effect, 0.15 fM miRNA and 20 nM ATP were simultaneously detected. With the proper signal amplification mode, the method can be extended to the sensitive and simultaneous detection of other biomarkers at different concentration levels, thereby enabling the developed method to be a universal sensing platform for a variety of target analytes.

EXPERIMENTAL SECTION

Materials and Reagents. All oligonucletides designed in this study were synthesized by Sangon Biotech Co., Ltd. (Shanghai China); their sequences are listed in Table 1. Magnetic microbeads (MBs) modified with carboxyl group (1.0−2.0 μm, 10 mg/mL) were commercially available from Baseline ChromTech Research Center (Tianjin, China). 1-Ethyl-3-(3-(dimethylamino)propyl) carbodiimide (EDC) and chloroauric acid ($HAuCl_4{\cdot}3H_2O$) were obtained from Sigma-Aldrich (St. Louis, MO). The washing buffer was phosphate-buffered saline (PBS) solution (10 mM phosphate buffer, 0.14 M NaCl, 2.7 mM KCl, pH 7.4). The HCR buffer was tris buffer (20 mM, pH 7.6) containing 300 mM NaCl and 50 mM $MgCl_2$. All chemicals employed were of analytical grade and used without further purification. Doubly distilled deionized water was used throughout the experiments. MCF-7 (human breast cancer cells), Ramos (B-cell, human lymphoma cells), and MCF-10A (human normal breast cell line) were obtained from Ocean University of China.

Apparatus. Transmission electron microscopy (TEM) images were taken with a JEM 1200EX transmission electron microscope (JEOL). UV−vis absorption spectra were obtained with a Cary 50 UV−vis−NIR spectrophotometer (Varian). SERS was performed on an inVia Raman microscope (Renishaw). HPLC analysis was performed in a Hitachi HPLC system (Hitachi). Real-time PCR assay was performed HiScript II One Step QRT-PCR SYBR Green Kit (Vazyme)

Preparation of Gold Nanoparticles (AuNPs). AuNPs were synthesized by reduction of tetrachloroauric acid ($HAuCl_4$) with trisodium citrate according to published protocols.[51,52] Briefly, 100 mL of 0.01% (w/w) $HAuCl_4$ solution was boiled with vigorous stirring, and then 1.5 mL

DOI: 10.1021/acs.analchem.5b01186
Anal. Chem. 2015, 87, 8242−8249

Scheme 1. Illustration of (A) the Asymmetric Signal Amplification SERS Assay and (B) Process of HCR

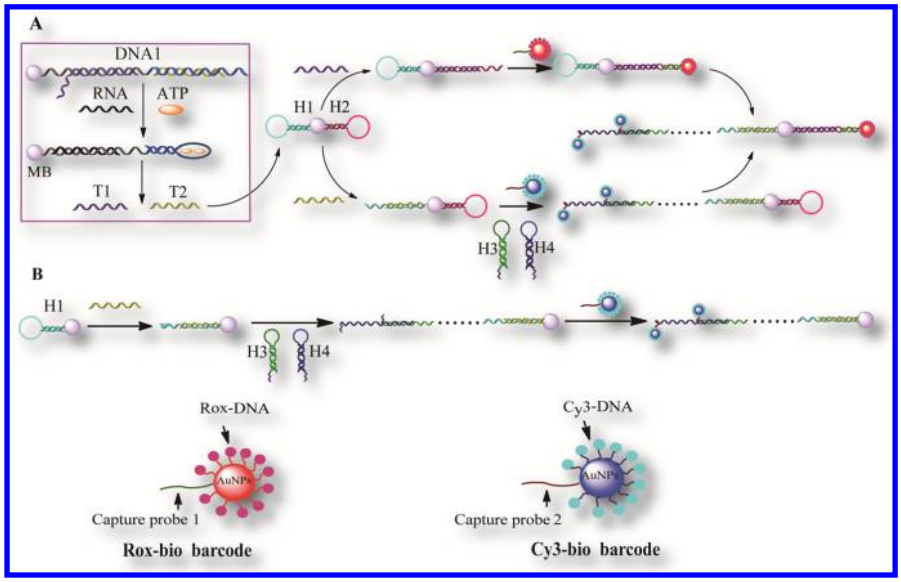

of 1% (w/w) trisodium citrate solution was rapidly added to the boiling solution. The resulting reaction solution was maintained at its boiling point for 30 min. The color of the solution changed from faint-yellow to purple before wine-red was reached, indicating the formation of AuNPs. The resulting colloidal suspension was allowed to naturally cool to room temperature with continuous stirring. The synthesis of AuNPs was characterized by TEM (Figure S-1). The prepared gold colloidal solutions were stored in brown glass at 4 °C until use.

Preparation of AuNP-Functionalized Raman Probes (Cy3-Bio Barcode and Rox-Bio Barcode). The Raman-probe functionized AuNPs were prepared as follows:[53] briefly, 10 μL of 1×10^{-7} M 5′-thiol modified capture DNA and 50 μL of 1×10^{-6} M biobarcode (5′-thiol and 3′-Rox or Cy3) was added to freshly prepared AuNPs (1 mL) and shaken gently overnight (approximately 20 h) at 37 °C. Subsequently, the DNA-AuNPs conjugates were aged in 0.05 M NaCl solution (200 μL) for 6 h and in 0.1 M NaCl solution (200 μL) for 6 h, respectively. Excess reagents were removed by centrifugation at 10000 rpm for 30 min. After the supernatant was removed, the red precipitate was washed and centrifuged three times. The resulting biobarcode probe was finally dispersed into 100 μL of 0.01 M pH 7.4 phosphate buffer (PBS, 0.01 M, pH 7.4) and stored at 4 °C.

Immobilization of Hairpin DNAs and DNA 1 onto MBs. H1 and H2 were heated to 90 °C for 5 min and then allowed to cool to room temperature for 1 h before use. First, a 20 μL suspension of carboxylated MBs was placed in a 0.5 mL Eppendorf tube (EP tube) and separated from the solution on a magnetic rack. After the MBs were washed three times with 200 μL of 0.1 M imidazol-HCl buffer (pH 6.8), they were activated in 200 μL of 0.1 M imidazol-HCl buffer (pH 6.8) containing 0.1 M EDC for 30 min at 37 °C. After being washed three times with 200 μL of 0.01 M PBS (pH 7.4), amino-group-modified DNA 1 (1 μM, 20 μL) and 20 μL of 1 μM H1 and 20 μL of 1 μM H2 were separately added to the freshly activated MBs and incubated at 37 °C overnight. Finally, the excess DNAs were removed by magnetic separation. The resulting DNA-conjugated MBs were rinsed three times with 200 μL of 0.01 M PBS (pH 7.4), resuspended in 200 μL of 0.01 M PBS and stored at 4 °C for use.

Assay Procedure of miRNA and ATP. The ATP and miR-203 analysis was carried out as follows: trigger 1 (T1) and trigger 2 (T2) were heated to 90 °C for 5 min and allowed to cool to room temperature for 1 h. First, single strand DNA 1 (1 μM, 20 μL), single strand T1 and T2 (2 μM, 20 μL) were added to the prepared aptamer-MB conjugates. After 1 h, the DNA-MB conjugates were washed three times with the washing buffer to remove the excess single strands. Then, miR-203 and ATP samples were added to the DNA-MB conjugates. After incubating for 1 h, the mixture of the supernatant DNA of MB was added to the hairpin DNA (H2 or H7)-MB conjugates and incubated with helper strands in Tris buffer (20 mM, pH 7.6) containing 300 mM NaCl and 50 mM $MgCl_2$ at 37 °C for HCR 2 h (or extracting solution from cancer cells with proper dilution). Then, placed in a magnetic rack, the excess helper DNA were removed by magnetic separation, followed by three washing with PBS. Then, the prepared AuNP-functionalized Raman Probes (Cy3-Bio Barcode and Rox-Bio Barcode) were added and incubated for 1 h, then applied to the surface of MB and allowed to hybridize with the immobilized hairpin DNAs (H2 or H7 with linear amplification) or the sticky ends of HCR product. Finally, the excess bio barcodes were removed by magnetic separation. The resulting MBs were rinsed three times with 200 μL of 0.01 M PBS (pH 7.4). Nonspecific binding Raman probes were washed out using PBS. The MBs-anchored SERS signal probes were resuspended in 50 μL of 0.01 M PBS prior to use.

SERS Measurements. Two microliters of the resulting MBs were pipetted onto the surface of gold film (glass slide with gold plating) and air-dried at room temperature. Raman spectra were measured using a Raman spectrometer at an excitation laser of 633 nm. The laser power was 5 mW. The acquisition time for each spectrum was 10 s. Three spectra were obtained from different sites of each sample and averaged to represent the SERS results, and the experiments were carried out in triplicate. Error bars show the standard deviation of the three experiments.

RESULTS AND DISCUSSION

Principle of the Asymmetric-Signal-Amplification SERS Assay. To simultaneously detect two biomarkers, miR-

DOI: 10.1021/acs.analchem.5b01186
Anal. Chem. 2015, 87, 8242−8249

203 and ATP, an asymmetric SERS signal amplification detection system based on a biobarcode probe and HCR was fabricated. In Scheme 1A, the asymmetric signal amplification was designed to include linear signal amplification with a biobarcode probe and quadratic signal amplification with HCR. The two signal amplifications respond to two different concentrations of analyte. Scheme 1 shows the design three types of functional units in the amplification system: target recognition, signal transduction, and amplification units. The first type of unit was a target recognition unit shown in the left column of Scheme 1, where the bifunctional probe is assembled and DNA1 is immobilized on a magnetic bead (MB) with binding to T1 and T2. DNA1 contains two main sections: a strand complementary to miR-203, and ATP aptamer. The second type of unit was a signal transduction unit, which consists of two types of hairpin DNA, H1 and H2, immobilized on MB. The third type of unit was signal simplification unit, which consists of two types of hairpin DNA (H3 and H4) as helper strands for HCR, two types of bio barcode. The two types of SERS biobarcode both were oligonucleotide-functionalized Au NPs, which were Cy3-bio barcode and Rox-bio barcode (Raman probe). Bio barcode consists of a large number of signal DNA (Cy3-DNA for Cy3-bio barcode or Rox-DNA for Rox-bio barcode) and capture DNA immobilized onto the Au NPs. The Au NPs simultaneously acted both as a Raman-signal-enhancing substrate and a Raman signal carrier. The Raman signals of Rox and Cy3 were in response to sample mixtures containing different concentrations of ATP and miR-203, respectively.

In the presence of miR-203, DNA1 bound to miR-203 and T1 was released to the solution by competition hybridization. T1 was complementary to the loop part of H1 immobilized on the MB, so it binded to H1 to open the hairpin structure of H1. The stem near to the 3′ end of H1 was unlocked to trigger the HCR reaction. As shown in Scheme 1B, the HCR mechanism employed the stem near to the 5′ end of H1 hairpin DNA (H1) as an initiator and two hairpins (H3 and H4) as helper strands. The key to this HCR system was the storage of potential energy in short loops protected by long stems. In the present HCR system, each hairpin was caught in a kinetic trap, preventing the system from rapidly equilibrating. Introduction of an initiator strand (the stem of H1) triggered a chain reaction of alternating kinetic escapes by the two hairpin species (H3 and H4) corresponding to "polymerization" into a nicked double helix. The sticky ends of H3 and H4 were complementary to the capture DNAs (C1) of Cy3-bio barcode (the sequence of the stick end is shown in Table 1), so abundance of SERS biobarcodes was attached to MB. As a result, miR-203 could be detected quantitatively by measuring the Raman signal of Cy3 attached on MB after quadratic signal amplification through the combination of the biobarcode and HCR after magnetic separation.

In the presence of ATP, the aptamer/target complex was formed with DNA1 binding to ATP, and T2 was entirely dissociated into solution upon aptamer/target binding event, T2, in turn, then activated the linear signal amplification with biobarcode signal amplification, which was complementary to the loop part of a hairpin probe (H2) immobilized onto the MB. The stem portion of the hairpin was opened, and the Rox-labeled SERS biobarcode probe was attached. ATP could be identified by measuring the Raman signal of Rox attached to the hairpin DNA on MB.

Because of the asymmetric amplification nature of the proposed strategy, the difference in SERS signal intensity among the low-concentration miRNA and high-concentration ATP is reduced. Thus, the detection precision is greatly improved. The proposed strategy is potentially universal because the sequences of the bifunctional probe can easily be designed to detect other biomarkers via changes in the corresponding aptamer.

Analytical Performance of the Asymmetric Signal Amplification SERS Assay. Under optimized conditions (the detail of optimization experiments in Supporting Information), mixtures of ATP standard and miR-203 standard at different concentrations were simultaneously determined. In Figure 1,

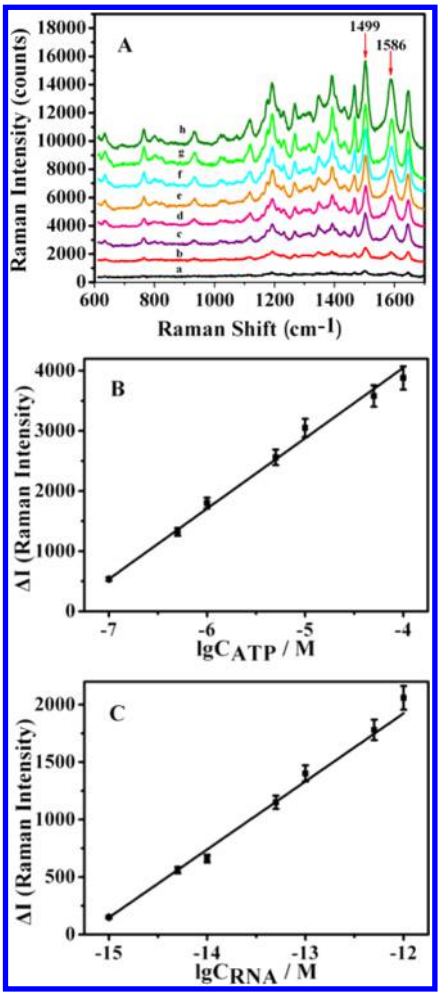

Figure 1. (A) SERS spectra for increasing concentrations of ATP (a, 0; b, 1.0×10^{-7}; c, 5.0×10^{-7}; d, 1.0×10^{-6}; e, 5.0×10^{-6}; f, 1.0×10^{-5}; g, 5.0×10^{-4}; h, 1.0×10^{-4} M) and miR-203 (a, 0; b, 1.0×10^{-15}; c, 5.0×10^{-15}; d, 1.0×10^{-14}; e, 5.0×10^{-14}; f, 1.0×10^{-13}; g, 5.0×10^{-13}; h, 1.0×10^{-12} M). (B) Variance of the Raman intensity normalized with the concentration of ATP. (C) Variance of the Raman intensity normalized with the concentration of miR-203.

the Raman signals of Rox and Cy3 are in response to sample mixtures containing different concentrations of ATP and miR-203. In the spectrum of the mixed probes in Figure 1A, characteristic peaks of both Rox (1344 and 1499 cm^{-1}, 1644 cm^{-1}) and Cy3 (1193 cm^{-1}, 1391 cm^{-1}, 1465 and 1586 cm^{-1}) are observed; the presence of these peaks indicates that these

DOI: 10.1021/acs.analchem.5b01186
Anal. Chem. 2015, 87, 8242−8249

Scheme 2. Illustration of (A) the Symmetric Linear Signal Amplification SERS Assay and (B) the Symmetric Quadratic Signal Amplification SERS Assay

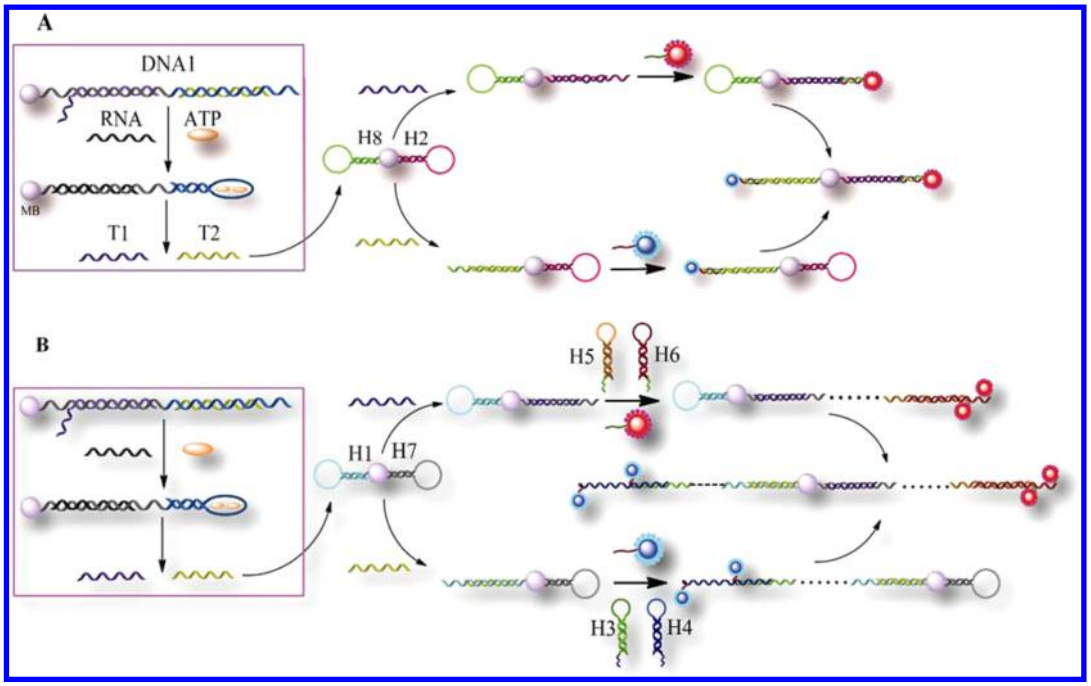

SERS probes could be used for simultaneous detection of two biomarkers.

In accordance with Figure 1A, the intensity of Raman scattering increased with increasing concentration of the corresponding target molecules, as indicated by the change in intensity of the characteristic peaks (1499 cm^{-1} for Rox and 1586 cm^{-1} for Cy3). As shown in Figure 1B, the calibration graph for ATP was linear in the range from 1×10^{-7} to 1×10^{-4} M with a detection limit of 2.0×10^{-8} M (S/N = 3); the calibration equation was calculated as $\Delta I_{Rox} = 1126.24 \lg C_{ATP} + 8487.09$ ($\Delta I_{Rox} = I - I_0$, where I is the Raman intensity in the presence of ATP and I_0 is the Raman intensity in the absence of ATP, C_{ATP} is the concentration of ATP), and the corresponding correlation coefficient (R) of calibration curve was 0.996, n = 7. A relative standard deviation (RSD) of 7.6% was obtained for 11 replicate measurements of 1.0×10^{-6} M ATP, suggesting good reproducibility of the assay. In Figure 1C, the calibration graph for miR-203 in concentrations range from 1×10^{-15} to 1×10^{-12} M was $\Delta I_{Cy3} = 592.52 \lg C_{miR\text{-}203} + 9035.18$ ($\Delta I_{Cy3} = I - I_0$, where I is the Raman intensity in the presence of miR-203 and I_0 is the Raman intensity in the absence of miR-203, n = 7; R= 0.997). The detection limit for miR-203 was as low as 1.5×10^{-16} M (S/N = 3).

Comparison of Different Signal-Amplification SERS Assays. For a proof-of-concept demonstration of the new asymmetric signal-amplification strategy, a series of control experiments were performed by employing two types of symmetric signal-amplification assays for ATP and miR-203 detection. The principle of two types of control assays is illustrated in the Supporting Information. The first type of symmetric signal amplification is a linear signal amplification based on SERS biobarcode probes (Scheme 2A). The second type of symmetric signal amplification: quadratic signal amplification based on SERS biobarcode probe and HCR (Scheme 2B). The analytical performances of two types of SERS assays were investigated. Series samples of ATP and miR-203 were determined by the present protocols. The results are shown in the Supporting Information (Figure S-5, Figure S-6).

In the first control assay with linear signal amplification, the detection limits for ATP and miR-203 were 1.6×10^{-8} and 3.9×10^{-11} M, respectively. Compared to asymmetric signal amplification SERS assay, the detection sensitivity of miR-203 was lower by 5 orders of magnitude. This lower sensitivity was attributed primarily to a low efficiency of linear symmetric signal amplification. In the second control assay with quadratic symmetric signal amplification, the detection limits for ATP and miR-203 were 5.6×10^{-9} and 1.2×10^{-14} M, respectively. Signals from ATP are saturated at the concentration of 10^{-6} M, so the ATP detection had a narrow linear range from 1×10^{-8} to 1.0×10^{-6} M. Compared to the detection sensitivity for miR-203 in the asymmetric signal amplification SERS assay, that in symmetric quadratic signal amplification was lower by approximately 2 orders of magnitude. Such a decrease of the sensitivity is attributable to two important factors. First, at the same time and the same condition, the detection range is from 10^{-8} to 10^{-5} M for ATP and 10^{-13} to 10^{-10} M for miRNA, with the concentration difference over 5 orders of magnitude. In the symmetric assay by the quadratic amplification, the high concentration of ATP resulted in a large amount of HCR product on the surface of MB. In Figure S-6B, signals from ATP were saturated in the concentration of 10^{-6} M. The large number of HCR product occupied the effective sensing interface of MB, with long double helix strands binding abundance of SERS biobarcodes for ATP. This led to a large steric hindrance and thus suppressed the capturing of the SERS probes with a low binding efficiency and rate of recognition unit for miR-203. Second, the signals of high-concentration target molecules often overlap the signals of lower expression analytes and contributed to a leveling effect of resolution.[24,25] However, in the asymmetric amplification assay, the different amplification modes respond to the markers with different concentration levels. A linear amplification mode responds to

DOI: 10.1021/acs.analchem.5b01186
Anal. Chem. 2015, 87, 8242−8249

high-concentration markers, and quadratic amplification mode responds to low-concentration markers. Although, the concentration of ATP was significantly higher than that of miR-203, there was no significant difference in the SERS intensity for ATP and miR-203.

To further verify the accuracy of the asymmetric signal amplification strategy, two control experiments for single analyte were performed for only ATP and miR-203 detection. As shown in Figure 2A, the intensity of Raman scattering increased with increasing concentration of ATP, when the asymmetric amplification assay was used. In Figure 2B, as indicated by the change in intensity of the characteristic peaks (1499 cm^{-1} for Rox), the calibration graph for ATP was linear in the range from 1.0×10^{-7} to 1.0×10^{-4} M. The calibration equation was calculated as $\Delta I_{Rox} = 1406.28 \lg C_{ATP} + 10817.17$ ($\Delta I_{Rox} = I - I_0$, where I is the Raman intensity in the presence of ATP, I_0 is the Raman intensity in the absence of ATP, and C_{ATP} is the concentration of ATP), and the corresponding correlation coefficient (R) of the calibration curve was 0.995, n = 7. As shown in Figure 2D, the calibration graph for miR-203 in the concentration range from 1.0×10^{-10} to 1.0×10^{-7} M was $\Delta I_{Cy3} = 779.16 \lg C_{miR\text{-}203} + 11821.89$ ($\Delta I_{Cy3} = I - I_0$, where I is the Raman intensity in the presence of miR-203 and I_0 is the Raman intensity in the absence of miR-203; n = 7; R = 0.994). As a result, the slope and intercept of the regression equation were close to those of the asymmetric amplification assay for simultaneous detection of two analytes, revealing a good agreement between both analytical methods. Simulation results show that the asymmetric amplification assay is suited for multiplex sensing of significant different levels of various biomolecules.

Therefore, the comparison of the multiplex capability of the different methods clearly indicates that the asymmetric signal amplification assay is more suited for multiplex sensing of significant different levels of various biomolecules.

Specificity of the Asymmetric Signal Amplification SERS Assay. To assess the specificity of the method for the simultaneous detection of ATP and miR-203, control experiments were performed by determining the same level of ATP and other small molecules in the nucleoside family [i.e., cytosine triphosphate (CTP), guanosine triphosphate (GTP), and uridine triphosphate (UTP)] as well as the same levels of miR-203 and some miRNA (e.g., miRNA-141 and miRNA-200b). The results are shown in Figure 3. Compared with the SERS signal obtained for ATP and miR-203, responses as low as that of the background were observed when other molecules were determined. These results indicate that the method provided good selectivity for its targets over the same level of nontarget molecules.

Real Sample Analysis of the Asymmetric Signal Amplification SERS Assay. To test the applicability of the developed method for ATP and miR-203 levels in real samples, ATP and miR-203 from different cell lines, MCF-7 (human breast cancer cells), Ramos (B-cell, human lymphoma cells) and MCF-10A (human normal breast cell line) were monitored by this method. From the results in Figure 4A, compared with the normal cell (MCF-10A), the current responses of ATP incubated the lysate from sample cells exhibit the over-expression in cancer cells (MCF-7 and Ramos), and the responses of miR-203 show the suppression in cancer cells, which is in good agreement with the previous report.[41−45] To assess the accuracy of this new method, we further compared asymmetric amplification SERS assay with high-performance liquid chromatography (HPLC) method for ATP and quantitative real time-polymerase chain reaction (RT-PCR) for miRNA in the samples. In Figure 4, the results obtained by the SERS assay shows an acceptable agreement with those obtained by HPLC and RT-PCR. The detailed description and data were added in Figures S7 and S8.

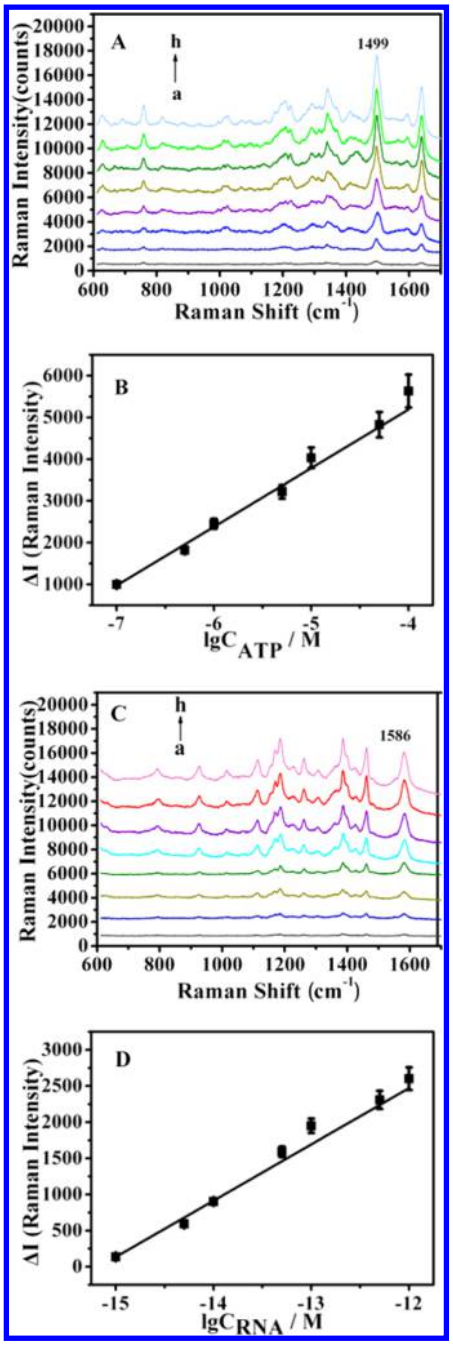

Figure 2. (A) SERS spectra for increasing concentrations of ATP (a, 0; b, 1.0×10^{-7}; c, 5.0×10^{-7}; d, 1.0×10^{-6}; e, 5.0×10^{-6}; f, 1.0×10^{-5}; g, 5.0×10^{-4}; h, 1.0×10^{-4} M). (B) Variance of the Raman intensity with the concentration of ATP. (C) SERS spectra for increasing concentrations of miR-203 (a, 0; b, 1.0×10^{-15}; c, 5.0×10^{-15}; d, 1.0×10^{-14}; e, 5.0×10^{-14}; f, 1.0×10^{-13}; g, 5.0×10^{-13}; h, 1.0×10^{-12} M). (D) Variance of the Raman intensity with the concentration of miR-203.

DOI: 10.1021/acs.analchem.5b01186
Anal. Chem. 2015, 87, 8242−8249

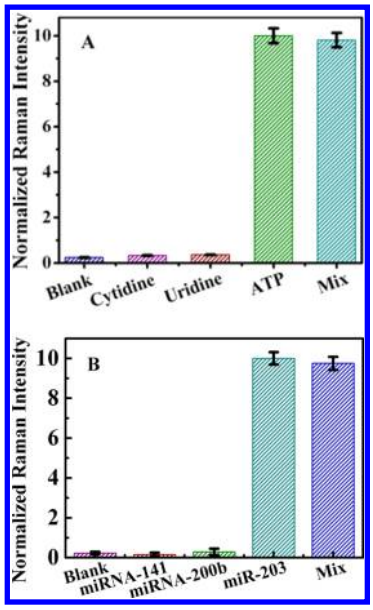

Figure 3. (A) Specificity for the detection of ATP against CTP, UTP, and GTP at a concentration of 1.0×10^{-6} M. (B) Specificity for the detection of miR-203 against miRNA 141 and miRNA-200b at 1.0×10^{-14} M.

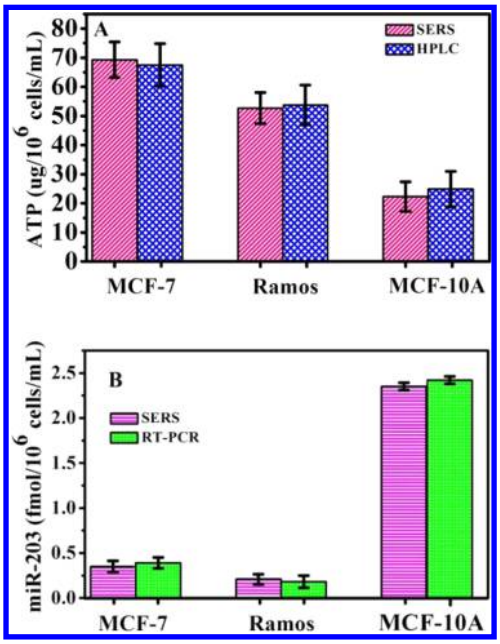

Figure 4. (A) Concentrations of ATP in sample cells measured by SERS (pink column) and HPLC (blue column). (B) Concentrations of ATP in sample cells measured by SERS (pink column) and RT-PCR (green column).

CONCLUSION

In conclusion, we have demonstrated a multiplexed and sensitive SERS sensing method for the simultaneous detection of significant different levels of biomarkers in the asymmetric signal amplification assay. With the use of the biobarcode probe and HCR signal amplification mode, the bifunctional probe is assembled to initiate asymmetric signal amplification, the linear signal amplification mode responds to high-concentration analytes, and the quadratic signal amplification mode responds to low-concentration analytes. With the use of this method, nanomolar ATP and femtomolar mRNA are simultaneously detected with high precision and the concentration difference over 11 orders. This strategy has been successfully employed in the simultaneous detection of cancer cellular ATP and miRNA and is a promising method for general use with significant different levels of various other biomolcules (biological cofactors, metabolites, and proteins).

ASSOCIATED CONTENT

Supporting Information

Additional information as noted in text. The Supporting Information is available free of charge on the ACS Publications website at DOI: 10.1021/acs.analchem.5b01186.

HPLC anaysis, RNA extraction and real-time PCR assay, characterization of gold nanoparticle (AuNPs), UV-visible spectra of the Rox-DNA and Cy3-DNA conjugates, optimization of the reaction temperature and pH, optimization of the HCR time, comparison of different signal-amplification SERS assays, calibration curve of ATP standards by HPLC detection, and quantitative real-time fluorescence monitoring of the qPCR reactions triggered by miR-203 (PDF)

AUTHOR INFORMATION

Corresponding Author

*E-mail: tangb@sdnu.edu.cn. Fax: +86 531 861800.

Notes

The authors declare no competing financial interest.

ACKNOWLEDGMENTS

This work was financially supported by the 973 Program (Grant 2013CB933800), the Natural Science Foundation of China (Grants 21227005, 21390411, 91313302, 21205065, and 21405087), the Postdoctoral Science Foundation of China (Grant 2012M521371), and Shandong Provincial Natural Science Foundation, China (Grant 2014ZRB019Y2).

REFERENCES

(1) Lu, J.; Getz, G.; Miska, E. A.; Alvarez-Saavedra, E.; Lamb, J.; Peck, D.; Sweet-Cordero, A.; Ebert, B. L.; Mak, R. H.; Ferrando, A. A.; Downing, J. R.; Jacks, T.; Horvitz, H. R.; Golub, T. R. *Nature* **2005**, *435*, 834−838.
(2) Tyagi, S. *Nat. Methods* **2009**, *6*, 331−338.
(3) Pritchard, C. C.; Cheng, H. H.; Tewari, M. *Nat. Rev. Genet.* **2012**, *13*, 358−369.
(4) Wang, G.; Lipert, R. J.; Jain, M.; Kaur, S.; Chakraboty, S.; Torres, M. P.; Porter, M. D.; Batra, R. E.; Porter, M. D. *Anal. Chem.* **2011**, *83*, 2554−2561.
(5) Bush, K. T.; Keller, S. H.; Nigam, S. K. *J. Clin. Invest.* **2000**, *106*, 621−626.
(6) Xiang, Y.; Lu, Y. *Anal. Chem.* **2012**, *84*, 4174−4178.
(7) Uludag, Y.; Tothill, I. E. *Anal. Chem.* **2012**, *84*, 5898−5904.
(8) Duan, R. X.; Zuo, X. L.; Wang, S. T.; Quan, X. Y.; Chen, D. L.; Chen, Z. F.; Jiang, L.; Fan, C. H.; Xia, F. *J. Am. Chem. Soc.* **2013**, *135*, 4604−4607.
(9) Yin, B. C.; Liu, Y. Q.; Ye, B. C. *J. Am. Chem. Soc.* **2012**, *134*, 5064−5067.
(10) Liu, H.; Li, L.; Duan, L.; Wang, X.; Xie, Y.; Tong, L.; Tang, B.; Wang, Q. *Anal. Chem.* **2013**, *85*, 7941−7947.
(11) Zhu, G.; Liang, L.; Zhang, C. Y. *Anal. Chem.* **2014**, *86*, 11410−11416.
(12) Liao, Y.; Huang, R.; Ma, Z.; Wu, Y.; Zhou, X.; Xing, D. *Anal. Chem.* **2014**, *86*, 4596−4604.

DOI: 10.1021/acs.analchem.5b01186
Anal. Chem. 2015, 87, 8242−8249

(13) Deng, R.; Tang, L.; Tian, Q.; Wang, Y.; Lin, L.; Li, J. *Angew. Chem., Int. Ed.* **2014**, *53*, 2389−2393.
(14) Wang, J.; Cao, Y.; Xu, Y. Y.; Li, G. X. *Biosens. Bioelectron.* **2009**, *25*, 532−536.
(15) Wu, J.; Fu, Z. F.; Yan, F.; Ju, H. X. *TrAC, Trends Anal. Chem.* **2007**, *26*, 679−688.
(16) Wilson, M. S.; Nie, W. *Anal. Chem.* **2006**, *78*, 6476−6483.
(17) Chen, T.; Wu, C. S.; Jimenez, E.; Zhu, Z.; Dajac, J. G.; You, M.; Han, D.; Zhang, X.; Tan, W. *Angew. Chem., Int. Ed.* **2013**, *52*, 2012−2016.
(18) Peng, X. H.; Cao, Z. H.; Xia, J. T.; Carlson, G. W.; Lewis, M. M.; Wood, W. C.; Yang, L. *Cancer Res.* **2005**, *65*, 1909−1917.
(19) Chon, H.; Lee, S.; Yoon, S. Y.; Chang, S. I.; Lim, D. W.; Choo, J. B. *Chem. Commun.* **2011**, *47*, 12515−12517.
(20) Li, N.; Chang, C. Y.; Pan, W.; Tang, B. *Angew. Chem., Int. Ed.* **2012**, *51*, 7426−7430.
(21) Wang, X.; Xia, Y. Q.; Liu, Y. Y.; Qi, W. X.; Sun, Q. Q.; Zhao, Q.; Tang, B. *Chem. - Eur. J.* **2012**, *18*, 7189−7195.
(22) Pan, W.; Zhang, T.; Yang, H.; Diao, W.; Li, N.; Tang, B. *Anal. Chem.* **2013**, *85*, 10581−10588.
(23) Nakano, S.; Fukuda, M.; Tamura, T.; Sakaguchi, R.; Nakata, E.; Morii, T. *J. Am. Chem. Soc.* **2013**, *135*, 3465−3473.
(24) Mohimen, A.; Dobo, A.; Hoerner, J. K.; Kaltashov, I. A. *Anal. Chem.* **2003**, *75*, 4139−4147.
(25) Falick, A. M.; Maltby, D. A. *Anal. Biochem.* **1989**, *182*, 165−169.
(26) Guo, Q. M. *Curr. Opin. Oncol.* **2003**, *15*, 36−43.
(27) Hoshi, S.; Kobayashi, S.; Takahashi, T.; Suzuki, K. I.; Kawamura, S.; Satoh, M.; Chiba, Y.; Orikasa, S. *Urology* **1999**, *53*, 228−235.
(28) Taton, T. A.; Mirkin, C. A.; Letsinger, R. L. *Science* **2000**, *289*, 1757−1760.
(29) Bernard, P. S.; Wittwer, C. T. *Clin. Chem.* **2002**, *48*, 1178−1185.
(30) Li, H.; Rothberg, L. J. *Anal. Chem.* **2004**, *76*, 5414−5417.
(31) Thompson, D. G.; Enright, A.; Faulds, K.; Smith, W. E.; Graham, D. *Anal. Chem.* **2008**, *80*, 2805−2810.
(32) Chan, W. C.; Nie, S. *Science* **1998**, *281*, 2016−2018.
(33) Gibbs, R. A. *Anal. Chem.* **1990**, *62*, 1202−1204.
(34) Wu, P. S.; Ozawa, C.; Lim, K. S.; Vasudevan, P. S. G; Dixon, N. E.; Otting, G. *Angew. Chem., Int. Ed.* **2007**, *46*, 3356−3358.
(35) Fire, A.; Xu, S. *Proc. Natl. Acad. Sci. U. S. A.* **1995**, *92*, 4641−4645.
(36) Strömberg, M.; Gomez de la Torre, T. Z.; Göransson, J. G.; Gunnarsson, K.; Nilsson, M.; Svedlindh, P.; Strømme, M. *Anal. Chem.* **2009**, *81*, 3398−3406.
(37) Cho, E. J.; Yang, L. T.; Levy, M.; Ellington, A. D. *J. Am. Chem. Soc.* **2005**, *127*, 2022−2023.
(38) Weizmann, Y.; Cheglakov, Z.; Pavlov, V.; Willner, I. *Angew. Chem., Int. Ed.* **2006**, *45*, 2238−2242.
(39) Guo, Q.; Yang, X.; Wang, K.; Tan, W.; Li, W.; Tang, H.; Li, H. *Nucleic Acids Res.* **2009**, *37*, e20.
(40) Xu, W.; Xue, X.; Li, T.; Zeng, H.; Liu, X. *Angew. Chem., Int. Ed.* **2009**, *48*, 6849−6852.
(41) Koshiol, J.; Wang, E.; Zhao, Y. D.; Marincola, F.; Landi, M. T. *Cancer Epidemiol., Biomarkers Prev.* **2010**, *19*, 907.
(42) Zhu, X.; Er, K.; Mao, C.; Yan, Q.; Xu, H.; Zhang, Y.; Shi, H.; et al. *Cell. Physiol. Biochem.* **2013**, *32*, 64−73.
(43) Campuzano, S.; Torrente-Rodríguez, R. M.; López-Hernández, E.; Conzuelo, F.; Granados, R.; Sánchez-Puelles, J. M.; Pingarrón, J. M. *Angew. Chem., Int. Ed.* **2014**, *53*, 6168−6171.
(44) Liu, Z.; Chen, C. S.; Liu, B.; Wu, J. P.; Zhou, Y. B.; He, L. Y.; Ding, J. S.; Liu, J. W. *Anal. Chem.* **2014**, *86*, 12229−12235.
(45) Wang, C.; Zheng, X. Q.; Shen, C. Y.; Shi, Y. R. *J. Exp. Clin. Cancer Res.* **2012**, *31*, 58.
(46) Degliangeli, F.; Kshirsagar, P.; Brunetti, V.; Fiammengo, R.; Pompa, P. P. *J. Am. Chem. Soc.* **2014**, *136*, 2264−2267.
(47) Zhang, Q.; Piston, D. W.; Goodman, R. H. *Science* **2002**, *295*, 1895−1897.
(48) Lin, S.-J.; Defossez, P. A.; Guarente, L. *Science* **2000**, *289*, 2126−2128.
(49) Bruzzone, S.; De Flora, A.; Usai, C.; Graeff, R.; Lee, H. C. *Biochem. J.* **2003**, *375*, 395.
(50) Wilkinson, A.; Day, J.; Bowater, R. *Mol. Microbiol.* **2001**, *40*, 1241−1248.
(51) Frens, G. *Nature, Phys. Sci.* **1973**, *241*, 20−22.
(52) Li, Y.; Lei, C. C.; Zeng, Y.; Ji, X. T.; Zhang, S. S. *Chem. Commun.* **2012**, *48*, 10892−10894.
(53) Li, Y.; Qi, X. D.; Lei, C. C.; Yue, Q. F.; Zhang, S. S. *Chem. Commun.* **2014**, *50*, 9907−9909.

DOI: 10.1021/acs.analchem.5b01186
Anal. Chem. 2015, 87, 8242−8249